Proceedings of the 11th Brazilian Congress of Thermal Sciences and Engineering -- ENCIT 2006
Braz. Soc. of Mechanical Sciences and Engineering -- ABCM, Curitiba, Brazil,- Dec. 5-8, 2006

Paper CIT06-0500

MOLTEN CARBONATE FUEL CELL: DYNAMIC NUMERICAL MODELING AND EXPERIMENTAL INVESTIGATION

Elisângela Martins Leal
Combustion and Propulsion Laboratory, National Institute for Space Research
Rod. Presidente Dutra, km 40, SP/RJ, Cachoeira Paulista, SP, 12.630-000
elisangela@lcp.inpe.br

Faryar Jabbari
Mechanical and Aerospace Engineering Department
University of California, Irvine, CA 92697
fjabbari@uci.edu

Jacob Brouwer
National Fuel Cell Research Center
University of California, Irvine, CA 92697
jb@nfcrc.uci.edu

Abstract. *In this paper, a detailed model incorporating simplified geometric resolution of a molten carbonate fuel cell (MCFC) with detailed and dynamic simulation of all physical, chemical, and electrochemical processes in the stream-wise direction is presented. The model was developed using mass and momentum conservation, electrochemical and chemical reaction mechanisms, and heat-transfer. Results from the model are compared with data from an experimental MCFC unit. Furthermore, the model was applied to predict dynamic variations of voltage, current and temperature in an MCFC as it responds to varying load demands. The voltage was evaluated by applying a model developed by Yuh and Selman (1991a, 1991b). The results show that the model can be used to predict voltage and dynamic response characteristics of an MCFC accurately and consistently for a variety of temperatures and pressures.*

Keywords. *Molten carbonate fuel cell, agglomerate model, heat transfer, experimental analysis, temperature and pressure dependence of electrochemical loss terms.*

1. Introduction

Molten carbonate fuel cells (MCFC) are currently used in commercial power-generation systems with proven high efficiency and low emissions performance. However, the dynamic operation of systems based on this emerging MCFC technology are complex and include, for example, the interaction between electrochemical, physical, chemical, and thermal (heat transfer) processes. Moreover, thermal management is especially important in the MCFC stack operation because potential corrosion and electrolyte vaporization, which degrade stack performance and life, are sensitive to temperature changes. Because of this sensitivity, high fidelity models that can accurately capture the dynamic behaviour of the fuel cell and identify the thermal gradients within the cell are highly desirable.

The molten carbonate fuel cell uses a molten salt electrolyte, which is generally a mixture of lithium and potassium carbonates. The electrolyte materials, which become molten at operating temperatures, are usually supported and wicked to cover electrode surfaces through use of a ceramic electrolyte support mesh (often $LiAlO_2$). Anode materials are typically Ni-Cr/Ni-Al alloys and cathode materials are comprised of lithiated NiO. At the cathode, oxygen reacts with carbon dioxide and electrons to form carbonate ions (Appleby, 1993):

$$0.5\,O_2 + CO_2 + 2\,e^- \rightarrow CO_3^{2-} \tag{1}$$

The carbonate ions flow through the electrolyte matrix from cathode to anode. At the anode, the carbonate ions are consumed by oxidation of hydrogen to form steam and carbon dioxide releasing electrons to the external circuit (Appleby, 1993):

$$H_2 + CO_3^{2-} \rightarrow H_2O + CO_2 + 2\,e^- \tag{2}$$

The overall reaction consists of the reaction between hydrogen and oxygen yielding water, electricity and heat. It is exothermic because of the negative enthalpy change and the incomplete conversion of fuel to electricity in the stack.

Several groups have investigated and advanced MCFC technology over the years. These groups include the Illinois Institute of Technology, Delft University, the Gas Technology Institute (formerly GRI), Ansaldo Ricerche, CRIEPI, and others (EG&G Technical Services, 2002). The most significant advancements and recent investments in MCFC technology have been from the governments of the U.S. and Japan and from FuelCell Energy Corporation (formerly Energy Research Corporation). FuelCell Energy Corporation is currently selling and installing 250 kW, 1.5 MW, and 3.0 MW power plants based on their MCFC technology (Fuel Cell Energy, 2006).

2. Model Formulation

The molten carbonate fuel cell (MCFC) studied here is presented in Fig. 1. The cell has a planar configuration with co-flow channel flows. It can be physically broken down into 5 distinct components: anode and cathode separator plates, electrolyte, and anode and cathode channels. The separator plates are used to provide structural support to the electrolyte mesh as well as to separate the anode and cathode channels. The electrolyte mesh is where chemical reactions occur and current and heat are generated. Although, the electrolyte is a complicated molten structure with a certain concentration of carbonate ions traveling through, it was modeled as a solid structure with no mass storage. The mass of the electrolyte accounts for the presence of ions and the reduction and oxidation reactions are assumed to happen at the surface of this solid. The channel flows are where the products and reactants are brought to and from the electrolyte surface. In the model, for the channels, all of the dynamic conservation equations (mass, species, momentum, and energy) are solved simultaneously. The simplified geometry that is included in the model breaks the cell into 10 equidistant nodes along the length of the cell as shown in Fig. 1. Previous nodal sensitivity studies have shown that 10 nodes are sufficient to capture the performance of an MCFC cell of the current size and shape (Roberts *et al.*, 2003).

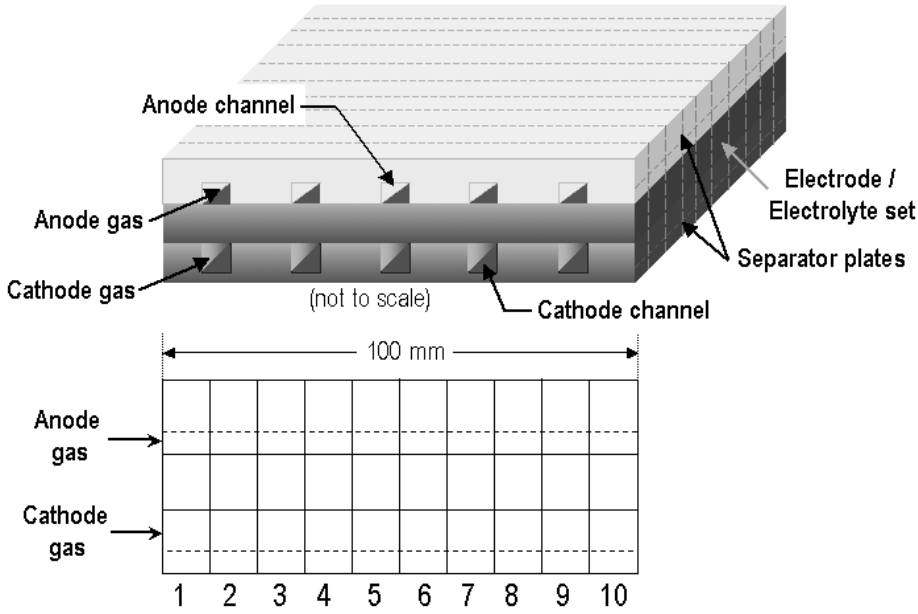

Figure 1. Schematic showing the geometry of the molten carbonate fuel cell dynamic model (Roberts *et al.*, 2003).

The electrochemistry in the cell is modeled as a quasi-steady process in which the chemical-kinetics is assumed to happen at a rate much faster than the transport and heat transfer dynamics. So, the reactions are assumed to happen instantaneously at the electrolyte surface. All of the polarization associated with slow reaction kinetics and/or slow diffusion times are incorporated into a local (i.e., nodal) bulk approximation of activation and concentration polarizations. As a result, no detailed electrochemical model that includes simulation of the charge transfer process or intermediate species is included and electrochemical reactions are assumed to be complete. With these assumptions, the species consumption and production rates become wholly dependant on the current produced from the cell. At any point in time then, the local current production depends upon local bulk species concentrations in the anode and cathode compartments, an iteratively determined cell voltage (using an electrode equi-potential assumption), and the local polarizations. A relatively simple mass/species balance equation for species conservation is thereby obtained (Gemmen *et al.*, 2000):

$$\forall\left(dC_j/dt\right) = N_{j,in} - N_{j,out} + R_p \tag{3}$$

2.1. Cell Voltage and Loss Mechanism

The electrical performance of a fuel cell in terms of temperature and gas compositions is given by the Nernst equation [8]:

$$E = E_0 + \frac{R_u T_e}{n F} \ln\left[\frac{p_{H_2,an} \left(p_{O_2,cat}\right)^{0.5}}{p_{H_2O,an}} \frac{p_{CO_2,cat}}{p_{CO_2,an}} \right] \tag{4}$$

The Nernst equation provides a relationship between the ideal standard potential (E_0) for the cell reaction and the ideal equilibrium potential for given local temperatures and partial pressures of reactants and products. Fuel cell irreversible losses are estimated through local (nodal) calculation of the three primary bulk losses of activation, concentration, and ohmic polarizations (Hirschenhofer *et al.*, 1998):

$$V_{cell} = E - \eta_{act} - \eta_{conc} - \eta_{ohm} \tag{5}$$

where V_{cell} is the cell voltage under load (V); η_{act} is the activation polarization (V); η_{conc} is the concentration polarization (V); and η_{Ohm} is the Ohmic polarization (V). Polarization losses are generally dependent on gas partial pressures, temperature, and current density, all of which are spatially distributed in an actual cell. Several approaches for calculating these polarization losses have been presented in the literature. One approach is to derive the activation polarization and the concentration polarization from the Butler-Volmer equation. Another approach, given by Yuh and Selman [1, 2], was selected for the current work. In this approach, the terms of activation polarization and concentration polarization are summed together to form one term for anode and one term for cathode as follows (Yuh and Selman, 1991a; 1991b):

$$(\eta_{act} + \eta_{conc}) = (\eta_{act} + \eta_{conc})_{an} + (\eta_{act} + \eta_{conc})_{cat} = \eta_{an} + \eta_{cat} \tag{6}$$

The polarizations at the anode (η_{an}) and cathode (η_{cat}) can then be written as, respectively (Yuh and Selman, 1991a; 1991b):

$$\eta_{an} = 2.27\times10^{-9} \exp\left(\frac{E_{act,an}}{T}\right) p_{H_2}^{-0.42}\ p_{CO_2}^{-0.17}\ p_{H_2O}^{-1.0} \tag{7}$$

$$\eta_{cat} = 7.505\times10^{-10} \exp\left(\frac{E_{act,cat}}{T}\right) p_{O_2}^{-0.43}\ p_{CO_2}^{-0.09} \tag{8}$$

The overall cell resistance (electronic and ionic) was expressed with the Arrhenius equation to calculate Ohmic polarization by (Koh *et al.*, 2001):

$$\eta_{ohm} = 0.45\times10^{-5} \exp\left[8600 \left(\frac{1}{T_e} - \frac{1}{923} \right) \right] \tag{9}$$

The pre-exponential factor in Eq. (9) was determined to be $0.45\text{x}10^{-5}$ Ω from measured experimental cell resistance data at 650ºC.

2.2. Energy balance and thermal properties

To perform the energy balance across the cell, the cell was separated into five distinct components as mentioned earlier: anode and cathode separator plates, anode and cathode channels, and the electrolyte matrix. These distinct components can be considered individual thermodynamic control volumes, each of which is simulated using a set of dynamic energy and heat transfer equations that account for sources/sinks and interactions amongst the components. Within the components, an energy equation was formulated by applying the first law of thermodynamics with heat transfer modeled by finite difference methods. To reduce simulation time, the fluid channels were modeled as control volumes with constant properties and a single unique temperature. Similarly, the electrolyte was also assumed to have constant properties and was modeled as one bulk component even though it consists of a molten carbonate salt mixture (sodium, potassium, or lithium salts) that is retained in a ceramic matrix of lithium aluminum oxide. For all the solid components, a lumped capacitance condition is assumed.

Due to the cell's planar configuration and operating conditions, stream-wise and normal to the top of the cell directions were assumed to be the primary directions of heat flux. This is because the largest exposed area is on the upper and lower surfaces of the cell and the thermal profile (due primarily to non-uniform heat generation) and convective fluxes are important in the stream-wise direction.

For the fluid channel, the energy equation is simultaneously solved with the momentum and species conservation equations, which were discussed earlier. For the fluid within the channel flow between the nodes, it was assumed that the mass that leaves or enters the control volume has a specific energy. Thus an energy balance can determine the bulk fluid temperature within each channel for every node. So, the energy equation can be written as (Achenbach, 1994):

$$\forall \frac{d(\rho E)}{dt} = \sum m_{in} E_{in} - \sum m_{out} E_{out} - Q_{conv,e} - Q_{conv,s} + P' \tag{10}$$

The separator plates are modeled as uniform-solid components with heat transfer to and from their boundaries. The separator plates have no thermal generation because there is no reaction within the separator plates; but since they are at the edge of the cell, energy can be extracted (lost to the environment from the fuel cell perspective). Practical MCFC systems, such as those employed by FuelCell Energy, may also deploy integrated reformers that can extract even more heat from the fuel cell in this manner. For the boundary conditions, the separator plates interact with ambient conditions (or neighboring cells if in a stack), with the adjacent fluid channel, and within neighboring separator plates. Applying an energy balance to the separator plates yields the following differential equation (Achenbach, 1994):

$$\frac{dQ}{dt} = -Q_{cond_{cs,s}} - Q_{conv_f} - Q_{conv_\infty} - Q_{cond_{cs,s-ele}} - Q_{ref} \tag{11}$$

The electrolyte energy equation is similar, however, heat generation terms appear to take into account the formation of water from the oxygen and hydrogen gases. Heat generation is assumed to occur within the electrolyte volume. In addition, the boundary conditions differ from the separator plates in that the electrolyte matrix is surrounded on both top and bottom channels so that only the immediate sides of the cell electrolyte are able to interact with the ambient conditions. The heat equation for the local bulk temperature in the electrolyte matrix that results is (Achenbach, 1994):

$$\frac{dQ}{dt} = -Q_{cond_e} - Q_{conv_{f,an}} - Q_{conv_{f,cat}} + Q_{cond_s} + Q_{gen} \tag{12}$$

Where:

$$Q_{gen} = i\left(\frac{\Delta H^f_{H_2O}}{n\,F} - V_{cell}\right) \tag{13}$$

The equations used for the conductive and convective heat transfer are of the form, respectively (Roberts *et al.*, 2003):

$$Q_{cond} = \frac{k\,A_{cond}}{L}\Delta T \tag{14}$$

$$Q_{conv} = h\,A_{conv}\Delta T \tag{15}$$

3. Discretization

In simulating the fuel cell, the cell is discretized along the stream-wise direction into ten distinct control volumes in order to capture variations along the length of the cell. Each control volume, or node, is comprised of an identical representation of the five cell components with the exception that the boundary conditions are provided by adjacent nodes or inlet/exit conditions. The stream-wise discretization allows the model to capture variations along the length of the cell as well as the potential for mass storage during dynamic operation.

When simulating a fuel cell, it is important to capture some of the geometrical features so that performance of cell can be accurately predicted. Even the overall cell performance depends upon local conditions and properties (temperature, pressure, species concentrations) that cannot be accurately captured without geometric resolution. In addition, some understanding or insight into local conditions can be valuable for determining whether the fuel cell is subjected to harmful or stressful conditions. However, full three-dimensional and dynamic resolution of the concurrent processes (e.g., chemistry and electrochemistry, heat transfer, mass transfer, momentum) is often computationally intensive. Thus, we have selected an approach that can capture essential geometrical features in a simplified manner allowing solution of the dynamic equations

that govern heat and mass transfer, momentum and energy conservation, chemistry and electrochemistry in the fuel cell. We also anticipate the use of this simplified approach can be readily included in a detailed dynamic fuel cell system model.

The cathode and anode channels are modeled by applying the conservation equations to the nodal control volumes. This allows for the solution of the state variables within the channels. Pressure is obtained by solving the momentum equation, which is an unsteady Bernoulli equation that assumes there is a time-varying, uniform bulk flow. In both channels mass and species balances are applied to the bulk flow. Flows are assumed to be ideal gases allowing the inlet bulk concentration to be easily obtained from local pressure and temperature. From inlet bulk flow and molar fractions, the species inlet concentrations can be determined. The inlet species concentrations are then used in a mass/species balance with reaction rates to form the relation dictating the exit molar fractions. Due to the Nernst term, there will be a spatial variation in the current generation since the fuel and oxidizer concentrations will decrease along the path of the flow. This ensures that a unique current distribution is achieved as a result of the simulation.

Along the length of the cell, a global equal-potential condition is enforced (Roberts *et al.*, 2003); that is the voltage across the cell throughout all nodes is constant and is also the cell voltage. As a result, at each node the following electro-chemical relation applies:

$$V_{cell} = \sum_{nodes} i_{node} R_{load} \tag{16}$$

Furthermore, the fuel cell is comprised of a one-dimensional array of nodes that are comprised of two-dimensional components, which yields an overall two-dimensional cell temperature distribution that is represented in Fig. 2. Figure 2 also presents the equivalent circuit heat transfer network of two adjacent nodes showing that the present model accounts for convective and conductive heat transfer between and amongst components as appropriate.

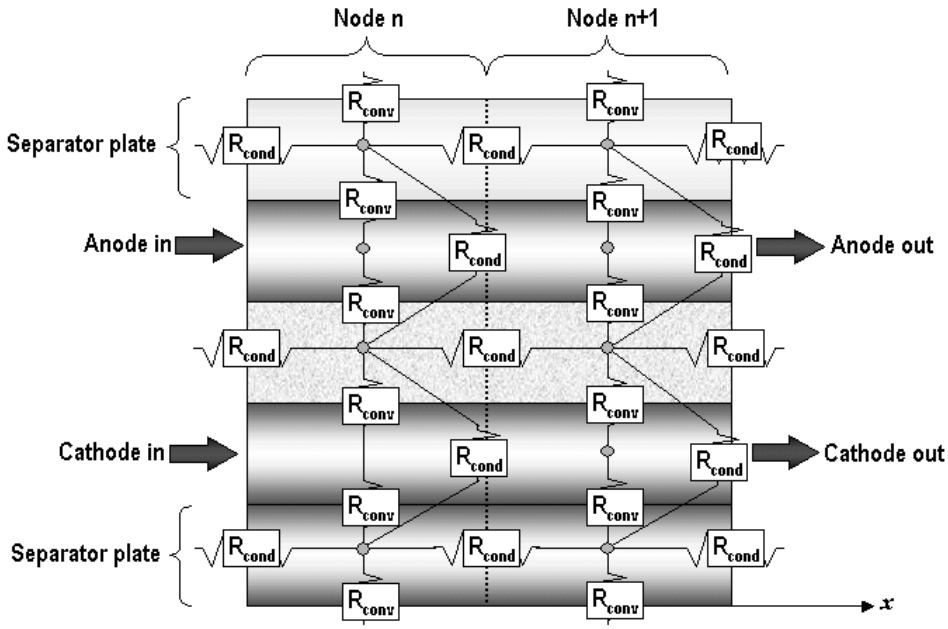

Figure 2. Schematic representation of heat transfer at the nodal level (Roberts *et al.*, 2003).

The current model was developed in MATLAB Simulink®, selected because of dynamic solution capabilities, a flexible and versatile user interface, and especially compatibility with dynamic control system development. The model is constructed in a physically representative manner, i.e., separate graphical components representing the anode, cathode, electrolyte, etc., for each of the model nodes. This allows for easy visualization and debugging.

4. Experimental investigation

An experimental investigation was conducted to measure the performance of a single MCFC cell. The experiments were designed to acquire data that could be useful for model validation. The MCFC tested has a planar area of 100 cm^2. The test stand clamped the actual cell between separator plates that were machined with 21 channels that are 3 mm in width and height for the cathode and 3 mm in width and 1.5 mm in height for the anode. This contributes to a relatively complex geometry for the solution of the heat transfer equations. The electrode-electrolyte matrix is sandwiched

between the two opposing separator plates and the fuel and oxidant flow is introduced into the opposing channels in a co-flow manner. A total cross-sectional area is calculated using actual cell geometry but features such as defects in the structural interconnections within the electrolyte structure itself and to the separator plates are ignored. The separator plates are modeled in a similar fashion as the electrolyte; as constant property flat plates that have no complex features with a cross-sectional area that is the same as the actual cell. For model validation, only 5 species are tracked in the anode and cathode channels during the experiments: CO_2, H_2, H_2O, N_2, and O_2 since these were the only gases used and measured in the experiments. Electric heaters were used to heat the fuel cell to a specified temperature because, unlike a fuel cell stack, a single cell is not capable of producing the heat necessary to self-sustained operation.

5. Results and discussion

The fuel cell parameters and operating conditions employed for the simulation are shown in Table 1. Table 2 presents the heat transfer coefficients and areas used in the model for the energy equations.

Table 1. Unit cell data and operating conditions for the MCFC dynamic model.

Parameter	Value
Number of channels	21
Operating pressure	101,325 Pa to 303,975 Pa
Operating temperature	860 K to 923 K
Anode channel height	0.0013 m
Cathode channel height	0.0032 m
Limiting current density	4,000 A/m^2
Transfer coefficient	0.5
Cell thickness	0.01 m
Separator plate thickness	0.0017 m
Separator plate density	7,900 kg m^{-3}
Separator plate heat capacity	611 J kg^{-1} K^{-1}
Electrolyte thickness	0.001 m
Activation energy in the anode	53,500 kJ $kmol^{-1}$
Activation energy in the cathode (P = 101,325 Pa and 923 K)	102,800 kJ $kmol^{-1}$
Activation energy in the cathode (P = 202,650 Pa and 923 K)	99,000 kJ $kmol^{-1}$
Activation energy in the cathode (P = 303,975 Pa and 923 K)	93,000 kJ $kmol^{-1}$
Inlet molar fraction of H_2 (anode)	0.60
Inlet molar fraction of CO_2 (anode)	0.15
Inlet molar fraction of H_2O (anode)	0.25
Inlet molar fraction of O_2 (cathode)	0.08
Inlet molar fraction of N_2 (cathode)	0.59
Inlet molar fraction of CO_2 (cathode)	0.08
Inlet molar fraction of H_2O (cathode)	0.25

Table 2. Parameters for the heat transfer equations in the model.

Conduction	k [W/m K]	A [m^2]	L [m]
Separator plate to separator plate (cathode)	25.4	0.000214	0.01
Separator plate to separator plate (anode)	25.4	0.000147	0.01
Separator plate to electrolyte (cathode)	25.4	0.000357	0.0031
Separator plate to electrolyte (anode)	25.4	0.000357	0.0013
Electrolyte to electrolyte	218	0.0001	0.01
Convection	**h [W/m^2 K]**	**A [m^2]**	
Separator plate to anode gas	83.86	0.0012	
Separator plate to cathode gas	92.96	0.0020	
Separator plate to ambient air			
top and bottom	10.00	0.0010	
Sides	10.00	0.0005	
Electrolyte to ambient air	21.00	0.0001	

5.1. Steady state performance comparison

The measured and predicted current-voltage curves are shown in Figs. 3 and 4 for the temperatures of 590ºC and 650ºC, respectively. These figures show results from the model as well as those obtained experimentally for three overall operating pressure conditions (1 atm, 2 atm, and 3 atm). These plots show primarily the kinetically dominated region for the MCFC (low current density). The results displayed in Fig. 3 show a maximum deviation in voltage between experiment and model results of about 3%, while those of Fig. 4 show a maximum deviation of only about 1.5%. This comparison of cell current-voltage performance is very good and well verifies the steady state model convergence to a reasonable solution. The comparisons shown in Fig. 4 are in especially good agreement with experimental data since some of the model parameters (e.g., overall cell resistance) were set by comparison to experimental data at 650ºC.

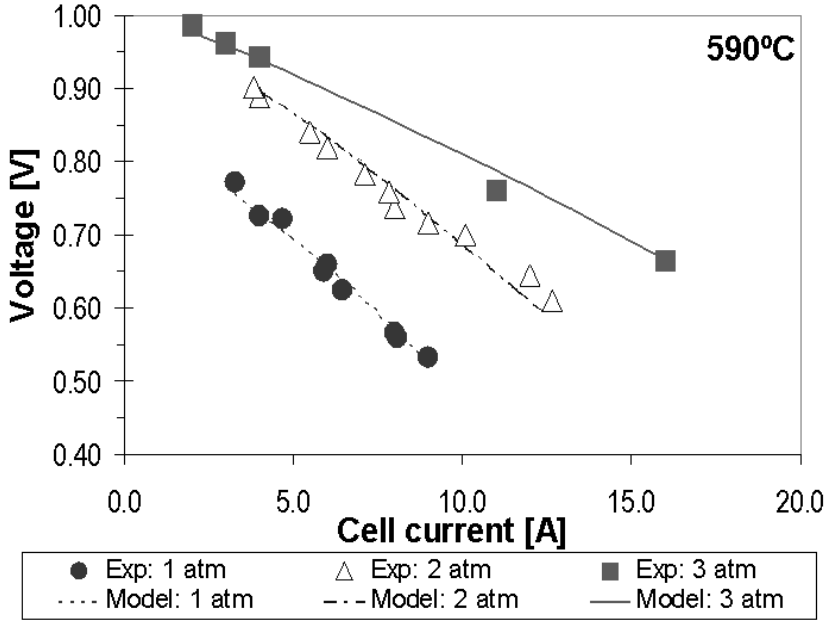

Figure 3. Voltage *versus* current for the experiment and model predictions at 590ºC.

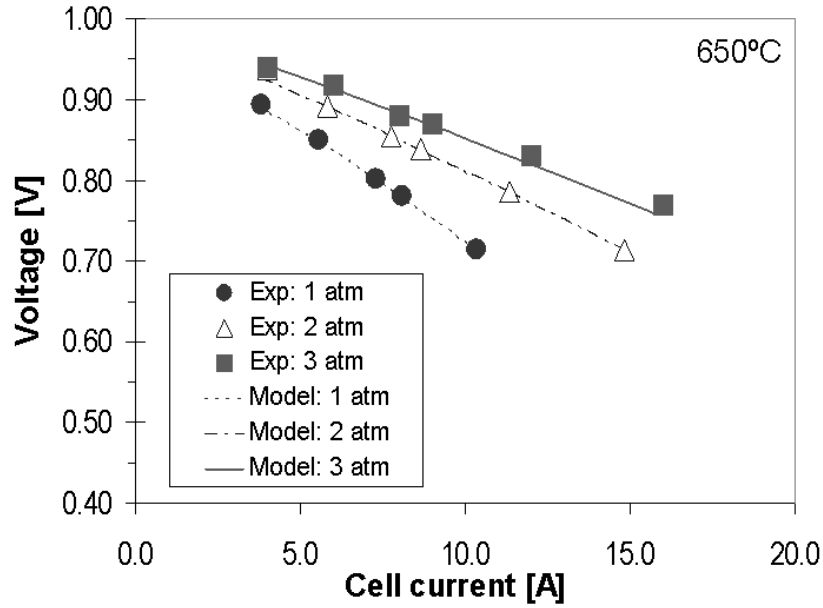

Figure 4. Voltage *versus* current for the experiment and model predictions at 650ºC.

5.2. Dynamic performance

Generally, when a fuel cell experiences a load change it responds with a quick electrochemical transient and a longer duration temperature transient and variation in space and time. Since most of the physical and chemical processes that govern fuel cell operation are strongly temperature dependent, the transient behavior of the cell voltage and current is expected to vary with the thermal transient. In a real system, these thermal transients can have long time constants (e.g., 100s – 1000s of seconds) due to the relatively large thermal mass of a fuel cell. In the current experiment, however, care was taken to control (and monitor) temperature within a narrow window of operation for all the results presented herein. This was accomplished with controllable heaters, thermocouples, and insulating materials that surrounded the fuel cell during tests. Thus the dynamic response of interest in the current study is one that accounts primarily for the electrochemical and transport controlled dynamics together with the small amount of temperature variations that occur along the length of the cell and for the cell overall during load perturbations.

The dynamic response of the MCFC cell was measured in the experiments for step changes in applied load resistance. Identical step changes in load resistance were applied in the simulations. In the simulations, the load of the cell was decreased from 0.1533 ohm to 0.0692 ohm, representing a decrease of about 55%, in order to determine the dynamic response of fuel cell voltage and current.

The behavior of current density along the length of the cell was investigated leading to similar current density profiles for operating temperature conditions of 590ºC and 650ºC. Figure 5 displays the distribution in current density for the temperature of 650ºC and pressure of 3 atm. In this figure for time < 2001 seconds the cell current density corresponds to the steady-state value for the initial load resistance. The asymptotic value for time > 2010 seconds corresponds to the new steady-state current density distribution. The intermediate period shows a fast initial increase in all nodes and for a subsequent smaller increase for upstream nodes (increase of about 8% for the first node) and a decrease for the downstream nodes (decrease of about 19% for the tenth node). The transient is due to the readjustment of the electrochemistry, material residence, and thermal response times. As voltage is enforced to be equal throughout the cell (Eq. 16), the Nernst potential has to be readjusted inside the model. However, hydrogen is more available for the first node than for the tenth because the anode reaction, which forces the model to readjust the current throughout the nodes.

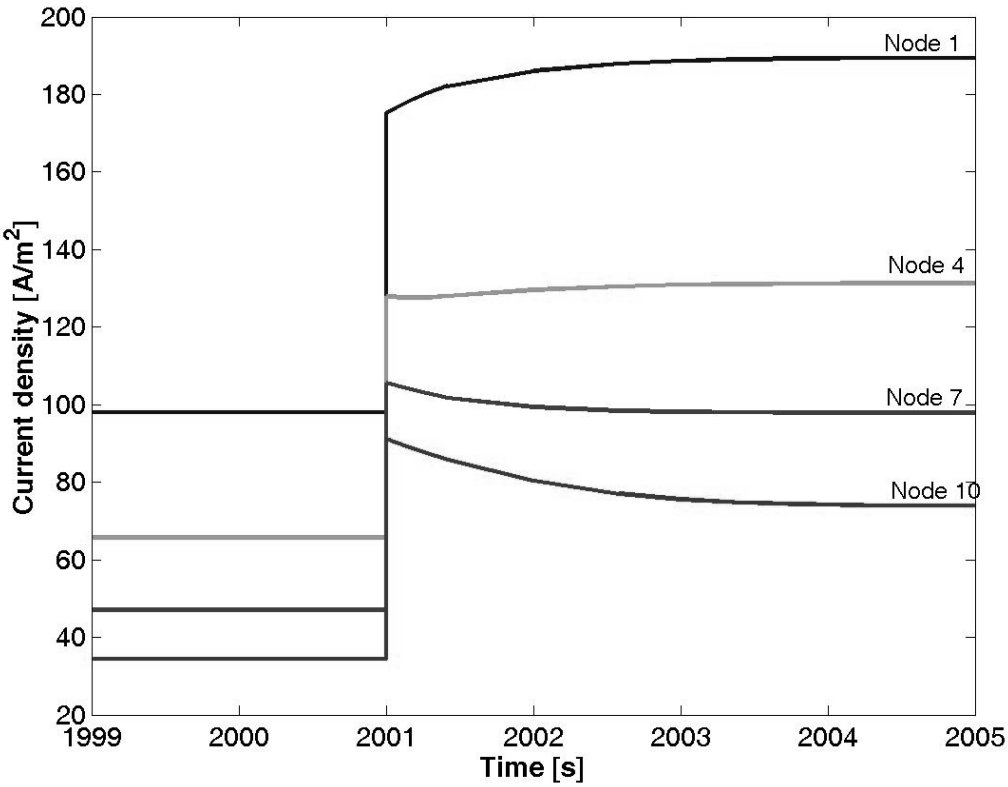

Figure 5. Dynamic response of cell current density during load resistance decrease (650ºC and 3 atm).

Figure 6 presents the transient response of fuel cell power (voltage times current) to the decreased load resistance perturbation 650ºC and 590ºC conditions. For 590ºC, the initial power increase is from 4.71 W to 7.61 W, representing an increase of about 62%. This is followed by a gradual decrease in power to approximately 7.48 W over a time period

of about 2 seconds. The new stead state condition corresponds to an overall power increase of about 59%. For 650ºC, the initial power increase is from 5.19 W to 9.83 W, representing an increase of about 89%. The final steady state for this temperature is approximately 9.58 W indicating an overall power increase of about 85%. The spike in the curves can be explained by the Nernst term adjustment in the model that initially produces a cell voltage that corresponds to the higher reactant concentration conditions of operation before the perturbation.

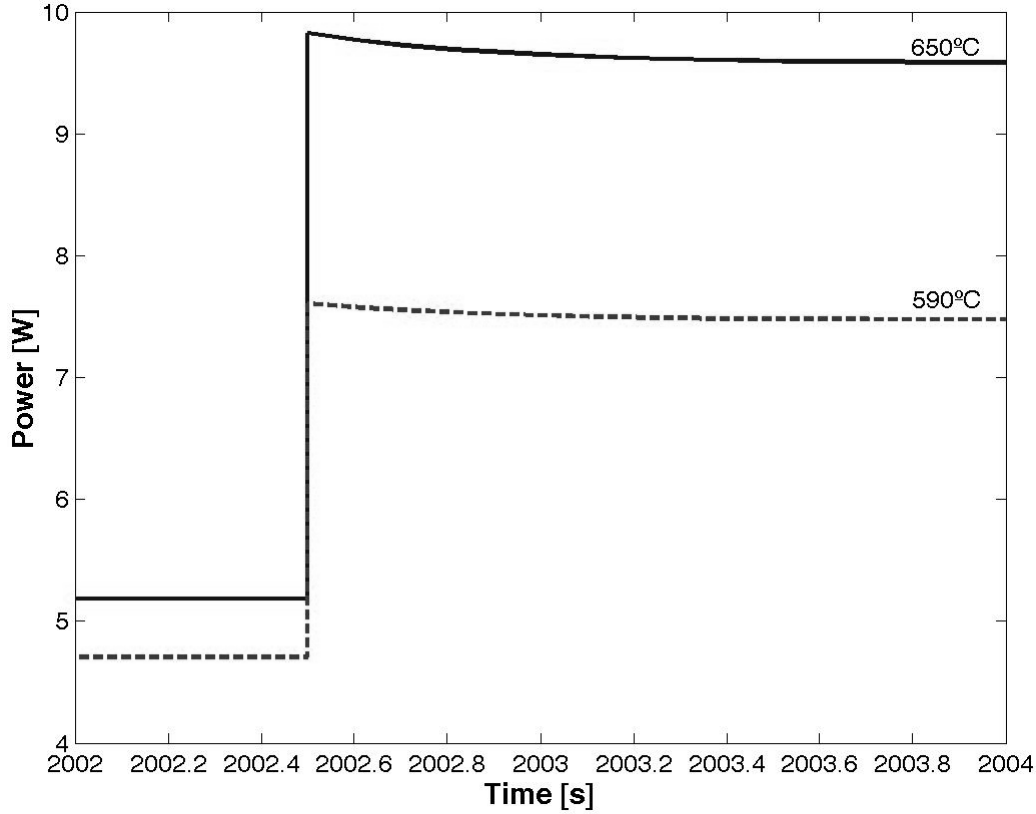

Figure 6. Effect of a load change on cell power (P = 2 atm).

Figure 7 shows the results for the hydrogen mole fraction in the anode gas stream versus time for several of the individual model nodes for the 650ºC case. As is seen in Figure 7, the upstream nodes have a relatively small H_2 concentration transient response. Downstream nodes, however, exhibit a change in H_2 concentration that results from the cumulative response of all upstream nodal H_2 consumption increases as indicated by the differences from node 1 to node 10.

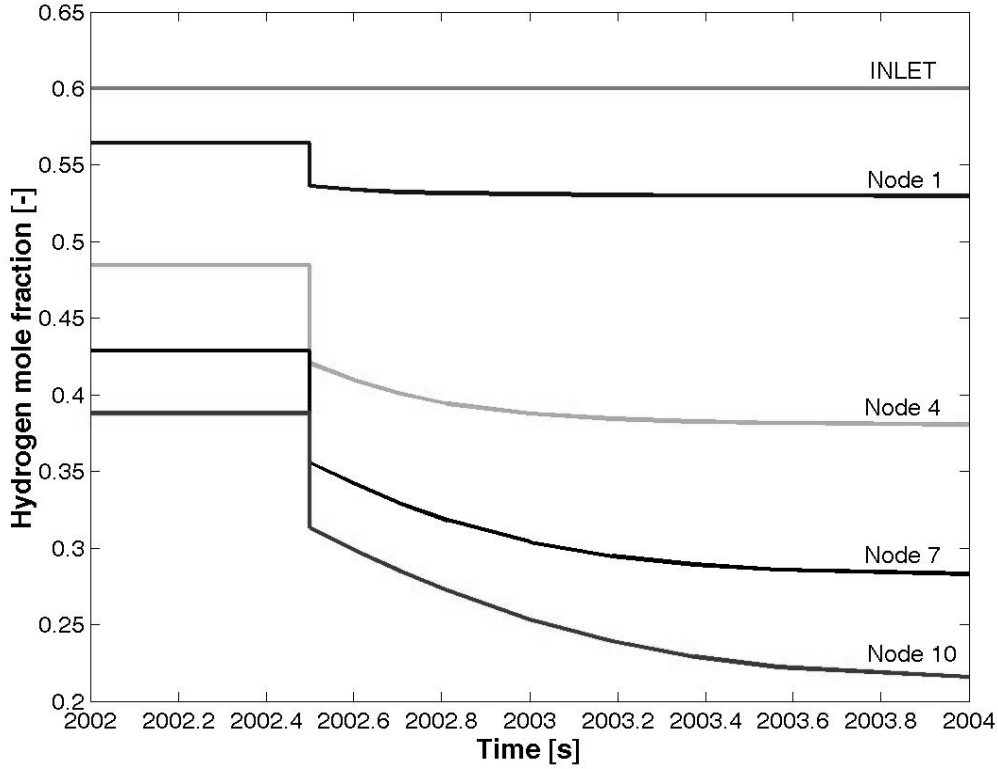

Figure 7. Transient hydrogen mole fraction during 55% load resistance.

6. Summary and Conclusions

Due to its high electrical efficiency, the molten carbonate fuel cell (MCFC) is an attractive candidate for decentralized power generation. However, the dynamic operation of systems based on this emerging MCFC technology are complex and include, for example, the interaction between electrochemical, physical, chemical, and thermal (heat transfer) processes. As a result, accurate and high fidelity models that can capture the dynamic behavior of the fuel cell and identify the thermal gradients within the cell are highly desirable.

In this work, a detailed model was developed in the MATLAB Simulink ® environment using the principles of fluid dynamics, electrochemical and chemical reaction mechanisms, and heat-transfer that govern a MCFC. A simplified 2-dimensional geometric representation of the cell is included. The model was applied to predict dynamic variations of voltage, current and temperature in an MCFC as it responds to varying load demands.

A corresponding set of experiments were carried out for a single MCFC cell using a test stand that can apply perturbations and measure the cell performance for a set of otherwise fixed operating conditions. The experiments were conducted in a manner to allow direct comparison to the dynamic simulation results. A series of simulations and analyses were carried out to verify model performance. The model is shown to provide steady state and dynamic simulation results that are in good agreement with experimental results.

The maximum steady state deviations between the model and experimental results were about 3%, for operating temperature conditions of 590ºC, and about 1.5%, for 650ºC. Furthermore, the effect of a fuel cell load increase and consequent voltage drop was simulated showing, for a 55% load resistance decrease at 650ºC and 3 atm, a power increase of about 83%. The dynamic response of current density along the cell length was revealed by the model with a maximum increase of about 8% for the upstream portions of the cell and a maximum decrease of about 19% for the downstream nodes in the immediate aftermath of the perturbation. The simulation results of the transient response of fuel cell power showed similar behavior for temperatures of 590ºC and 650ºC with an overall power increase of about 60% for the first and 85% for the latter, and a spike in the curves due to the Nernst term adjustment in the model. Furthermore, the perturbation in load showed for the hydrogen mole fraction changes in the nodes that downstream nodes exhibit cumulative response of all upstream nodal H_2 consumption. The transient responses in the fuel cell provide valuable insight into the operating characteristics of an MCFC.

These analyses demonstrate that first principles simulation using simplified cell geometry can be useful for garnering insight into the dynamic response characteristics and behavior of fuel cells. Future use of such verified simple models may be especially valuable in detailed system simulations for controls development.

7. Acknowledgments

We acknowledge the support of the California Energy Commission, which partially supported the development of a dynamic MCFC model. We also acknowledge the support of the National Energy Technology Laboratory, which donated the test stand used in the experiments and contributed to the model development. The first author thanks the financial support provided by FAPESP (Fundação de Amparo a Pesquisa do Estado de São Paulo, processo 2005/55375-2).

8. Legal Notice

9. References

Yuh, C.Y., Selman, J.R., 1991a, "The polarization of molten carbonate fuel cell electrodes. I. Analysis of steady-state polarization data", Journal of the Electrochemical Society, 138 (12), pp. 3642 - 3648.

Yuh, C.Y., Selman, J.R., 1991b, "The polarization of molten carbonate fuel cell electrodes. II. Characterization by AC impedance and response to current interruption", Journal of the Electrochemical Society, 138 (12), pp. 3649 - 3655.

Appleby, A. J., 1993, Chapter 5, In: L. J. M. J. Blomen and M. N. Mugerwa (eds), Fuel Cell Systems, Plenum Press, New York.

EG&G Technical Services, Inc., 2002, Science Applications International Corporation. Fuel Cell Handbook (sixth edition). DOE/NETL-2002/1179 Under Contract No. DE-AM26-99FT40575 U.S. Department of Energy, Office of Fossil Energy, National Energy Technology Laboratory.

Fuel cell Energy company. Available at http://www.fce.com/, last update 03/2006.

Roberts, R. A., Jabbari, F., Brouwer, J., Samuelsen, G. S. Liese, E. A., Gemmen, R. S., 2003, "Inter-laboratory dynamic modeling of a carbonate fuel cell for hybrid application", In: International Gas Turbine Institute Meeting of the ASME. Atlanta, Georgia.

Gemmen, R. S., Liese, E. A., Rivera, J. G., Jabbari, F., Brouwer, J., 2000, "Development of dynamic modeling tools for solid oxide and molten carbonate hybrid fuel cell gas turbine systems", In: 2000 ASME Turbo Expo, Munich, Germany.

Hirschenhofer, J. H., Stauffer, D. B., Engleman, R. R., Klett, M. G., 1998, Fuel cell handbook. US, Department of Energy.

Koh, J. H., Kang, B. S., Lim, H. C., 2001, "Analysis of temperature and pressure fields in molten carbonate fuel cell stacks", AIChe Journal, 47 (9), pp. 1941 – 1956.

Achenbach, E., 1994, "Three-dimensional and time-dependent simulation of a planar solid oxide fuel cell stack". Journal of Power Sources, 49, pp. 333 – 348.

Simulink/MATLAB is a product of The Mathworks, 3 Apple Hill Drive, Natick, MA 01760-2098, USA. (http://www.mathworks.com/).